

Article

Selective Oxidation of Furfural at Room Temperature on a TiO₂-Supported Ag Catalyst

Achraf Sadier , Sébastien Paul  and Robert Wojcieszak 

Univ. Lille, CNRS, Centrale Lille, Univ. Artois, UMR 8181–UCCS–Unité de Catalyse et Chimie du Solide, F-59000 Lille, France; sebastien.paul@centralelille.fr

* Correspondence: achraf.sadier@outlook.com (A.S.); robert.wojcieszak@univ-lille.fr (R.W.);
Tel.: +33-(0)-320336708 (R.W.)

Abstract: The catalytic performance of the Ag/TiO₂ catalyst was evaluated in the oxidation of furfural (FF) to furoic acid (FA) in an alkaline aqueous solution under 15 bar of air in a batch reactor. The catalytic activity, yield, and stability of the catalyst were compared as a function of different reaction parameters including temperature (25–110 °C), nature of the atmosphere, base equivalent ($n_{\text{base}}/n_{\text{FF}} = 0.25\text{--}3$), and nature of the inorganic bases used (NaOH, NaHCO₃, and Na₂CO₃). Under optimum conditions, the yield of FA (96%) was achieved at room temperature, with an excellent carbon balance (>98%). The recyclability of the catalyst was also studied and the catalytic activity of the Ag/TiO₂ catalyst slightly declined due to an increase in particle size as confirmed by TEM studies.

Keywords: furfural; oxidation; Ag nanoparticles; TiO₂; supported catalysts; liquid phase



Citation: Sadier, A.; Paul, S.; Wojcieszak, R. Selective Oxidation of Furfural at Room Temperature on a TiO₂-Supported Ag Catalyst. *Catalysts* **2022**, *12*, 805. <https://doi.org/10.3390/catal12080805>

Academic Editor: Alain Roucoux

Received: 5 July 2022

Accepted: 20 July 2022

Published: 22 July 2022

Publisher's Note: MDPI stays neutral with regard to jurisdictional claims in published maps and institutional affiliations.

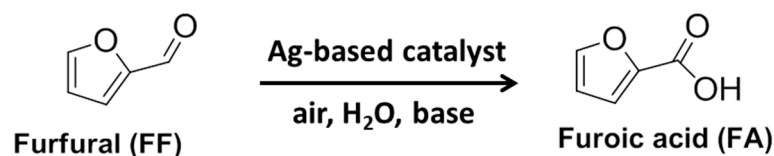


Copyright: © 2022 by the authors. Licensee MDPI, Basel, Switzerland. This article is an open access article distributed under the terms and conditions of the Creative Commons Attribution (CC BY) license (<https://creativecommons.org/licenses/by/4.0/>).

1. Introduction

Over the last decades, society has tended towards the use of the lignocellulosic biomass as an interesting alternative for the production of biofuels and chemicals [1–4]. According to the US department of energy (DOE), furfural (FF) is considered as one of the ten most relevant building platform molecules among the lignocellulosic biomass derivatives [5–7]. Xylan-rich hemicelluloses are sources of FF which can be further valorized by different methods including hydrogenation, aldol condensation, and oxidation into various key products [7,8]. In particular, the production of furoic acid (FA) through the selective oxidation of FF (Scheme 1) has drawn attention due to its potential application in the polymer industries as a precursor of 2,5-furandicarboxylic acid (FDCA) [9,10]. It is also used as starting material in the pharmaceutical, fragrance, agrochemical, and flavor industries [11,12]. The industrial production of FA from FF is generally performed using strong oxidizing agents via a Cannizzaro reaction, followed by the addition of H₂SO₄ as an acidification step [13]. This process is undesirable due to the corrosive and toxic nature of the employed reagents [12,14]. However, the application of heterogeneous catalysts in the presence of “green” oxidants such as H₂O₂, O₂, or air to improve the efficiency of oxidation reaction has been investigated [15]. Various noble metals such as Au, Pd, and Pt have been considered for the catalytic oxidation of FF to FA. Au-based catalysts have been considered so far as the most efficient for the partial oxidation of FF under green conditions [11,15–18]. Despite its high catalytic activity, the major drawback of gold in terms of cost and sustainability makes it attractive to search for alternative metals. There are few studies reporting the use of Ag, which has a much lower price than gold and its availability is confirmed by the huge world reserves. Sha et al. investigated the oxidation of FF into FA (92% yield) in an alkaline medium at 70 °C in the presence of a Ag₂O/CuO catalyst [19]. Recently, the oxidation of 5-(hydroxymethyl) furfural (HMF) to 5-hydroxymethyl-2-furancarboxylic acid (HMFA) over a Ag/ZrO₂ catalyst at 50 °C in the presence of air and NaOH as a base was studied. After 5 h and one equivalent of NaOH, 100% HMF conversion and 94% HMFA yield was

obtained [20]. Commercial TiO₂-P25 was used as a support with a non-basic character. It is stable in water under oxidation conditions [21].



Scheme 1. Oxidation of furfural (FF) into furoic acid (FA).

Herein, a monometallic Ag/TiO₂ catalyst was investigated for the selective oxidation of FF to FA at room temperature in an alkaline aqueous solution using air. The influence of the reaction parameters (e.g., temperature, atmosphere, ratio of base, and nature of base) on catalytic activity, yield, and carbon balance were also studied.

2. Results and Discussion

The physicochemical properties (chemical composition, specific surface area) of the synthesized Ag/TiO₂ catalyst were studied. Using the ICP-OES analysis, 6 wt.% loading of Ag was confirmed. The specific surface area of the Ag/TiO₂ catalyst was slightly lower (48 m² g⁻¹) compared to that of the fresh TiO₂ support (P25, 53 m² g⁻¹). The XRD patterns Ag/TiO₂ catalyst are compared to that of the pristine support in Figure 1. The XRD patterns of TiO₂ support confirmed the presence of a mixture of two known anatase and rutile phase structures. Contrary to that, the Ag/TiO₂ sample exhibited additional diffraction peaks (other than those of the supports) at 44°, 64°, and 77° which were attributed to silver in a metallic state. However, due to the overlapping of the main diffraction peak of metallic silver with the diffraction peak of TiO₂ at 38° (Figure 1), the particle size was estimated through TEM analysis.

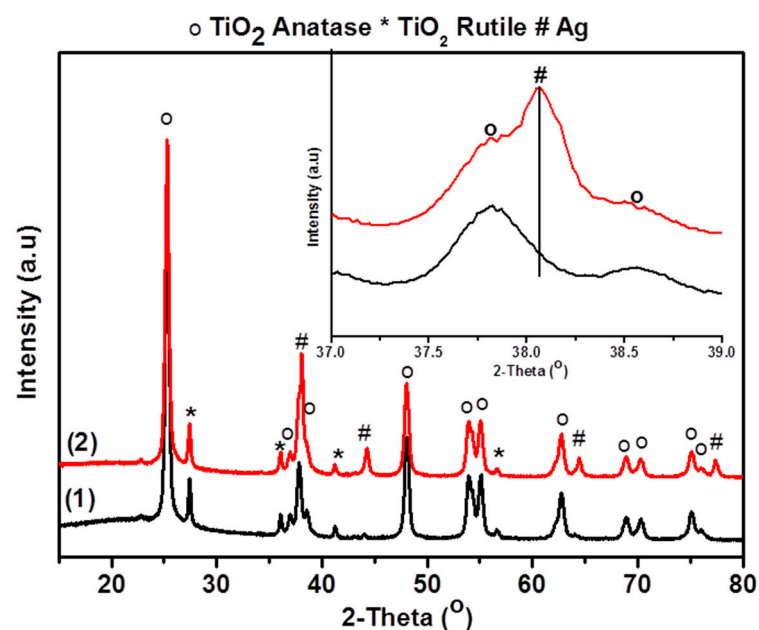


Figure 1. XRD patterns for TiO₂ (1), and Ag/TiO₂ (2).

The TEM image of the Ag/TiO₂ catalyst and its corresponding particle size histogram are shown in (Figure 2). In order to estimate the average particle size, approximately 200 particles were measured. The average particle size in Ag/TiO₂ was estimated to be 1.82 nm. This confirmed the obtention of a very good dispersion of silver nanoparticles on the support surface.

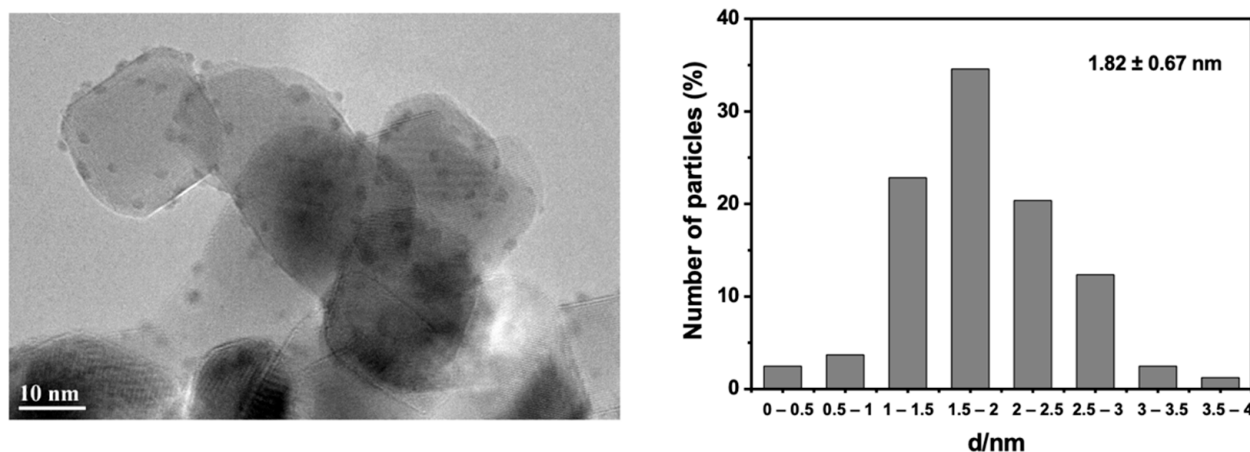


Figure 2. Representative TEM images and size distributions of the Ag/TiO₂ catalyst.

2.1. Effect of the Temperature

The effect of reaction temperature was investigated over the 25–110 °C range under 15 bar of air in the presence of Ag/TiO₂ catalyst. The evolution of FF concentration as a function of time is presented in Figure 3a and the yield of FA accompanied with carbon balance is shown in Figure 3b. At 25 °C, 96% conversion was achieved after 3 h of reaction. As expected, the higher the reaction temperature, the faster the reaction rate. For example, at 50 °C, an FF conversion of 93% was attained after 2 h, whereas 1.7 and 1 h were needed to reach the same conversion at 80 and 110 °C, respectively. When the reaction temperature was increased from 25 to 110 °C, the yield of FA significantly decreased from 96 to 45%, respectively (Figure 3b). The degradation of furfural through the formation of humins and humic acids occurred at a higher temperature (110 °C) resulting in a low carbon balance (45%) [15,17]. No leaching of silver was detected by ICP analysis of the liquid solution at the end of the reaction over the 25–110 °C range of temperature. Finally, a temperature of 25 °C was chosen for further experiments to avoid the formation of by-products due to the degradation and to keep a high carbon balance (>98%).

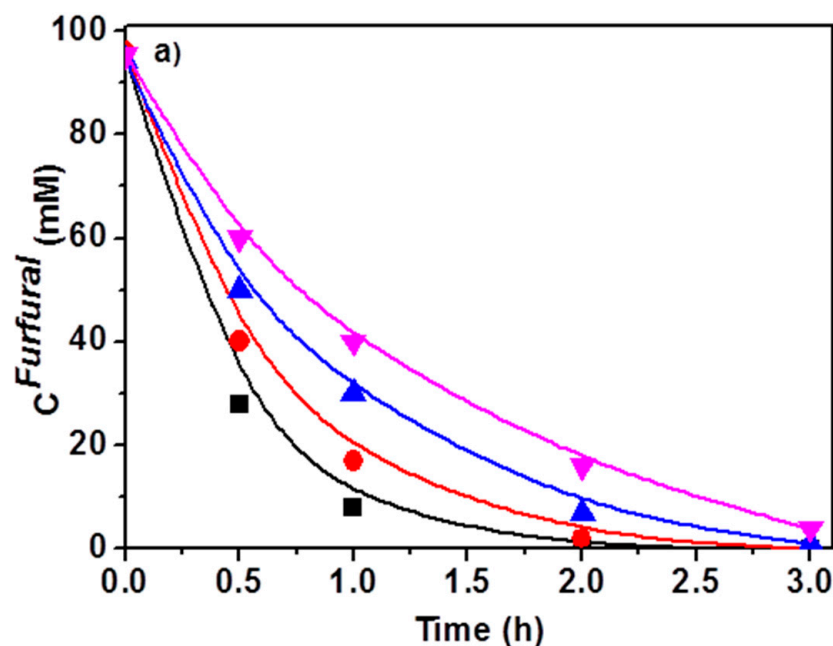


Figure 3. Cont.

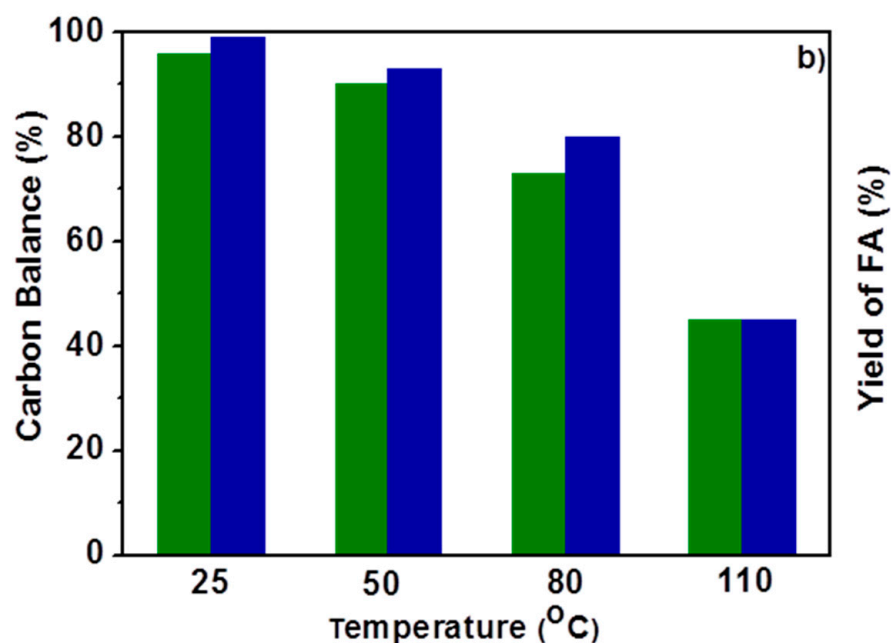


Figure 3. Effect of temperature on (a) temporal evolution of FF, (■) 110 °C; (●) 80 °C; (▲) 50 °C; (▼) 25 °C; (b) FA yield and carbon balance. (■) Yield to FA; (■) Carbon balance: Reaction conditions: 11.5 mg Ag/TiO₂, $n_{\text{FF}}/n_{\text{Ag}} = 300$, $C_{0(\text{FF})} = 0.1 \text{ mol L}^{-1}$, $n_{\text{OH}^-}:n_{\text{FF}} = 1$, 15 bar of air, 600 rpm. Three h reaction for (b).

2.2. Effect of the Atmosphere

Figure 4 shows the catalytic activity of a Ag/TiO₂ catalyst under air and N₂ atmosphere at 25 °C with one equivalent of NaOH. It can be seen that oxygen strongly influenced the furfural conversion. Under an inert gas atmosphere (N₂, 15 bar), the maximum conversion of furfural (14%) was rapidly reached after 1 h of reaction and it remained constant (maximum of 17% after 3 h). In the presence of an oxidative atmosphere, total furfural conversion was reached under 15 bar of air and 80% of furfural was converted under atmospheric pressure after 3 h (Figure 4). Selectivity remained optimal to furoic acid (~96%) whatever the atmosphere used.

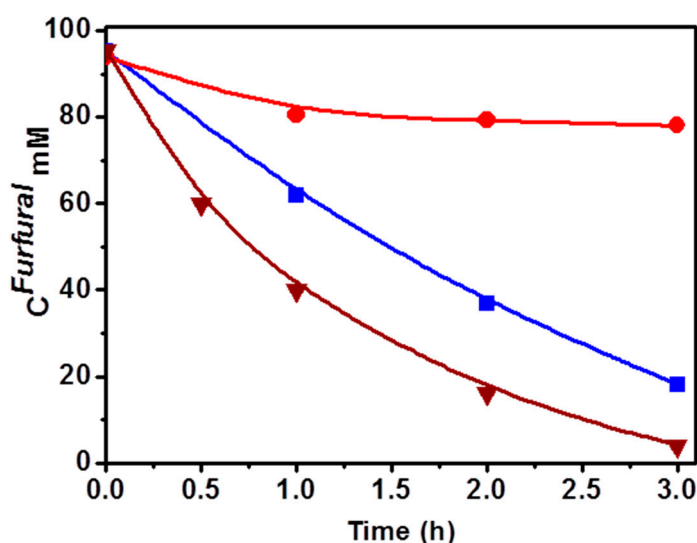


Figure 4. Effect of atmosphere on FF conversion and FA yield over Ag/TiO₂ catalyst. (●) 15 bar of nitrogen; (■) atmospheric pressure; (▼) 15 bar air. Reaction conditions: 11.5 mg Ag/TiO₂, $n_{\text{FF}}/n_{\text{Ag}} = 300$, $C_{0(\text{FF})} = 0.1 \text{ mol L}^{-1}$, $n_{\text{OH}^-}/n_{\text{FF}} = 1$, $T = 25 \text{ °C}$, 600 rpm.

A reaction mechanism was proposed in order to explain the difference in catalytic activity (Figure 5). First, in an alkaline aqueous solution, the aldehyde group of furfural directly undergoes a reversible hydration through nucleophilic attack of a hydroxide ion (OH^-) to the carbonyl group followed by proton transfer (from water) to the alkoxide ion intermediate. In the second step, the intermediate diol is dehydrogenated on the surface of reduced silver particles and forms furoic acid. During the catalytic cycle, the surface of silver is covered with adsorbed H-species that are removed by oxygen leading to the regeneration of the silver catalyst [22].

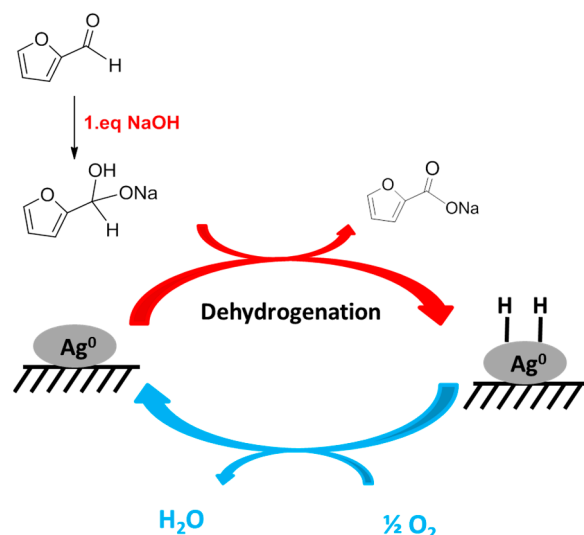


Figure 5. Schematic reaction mechanism of furfural oxidation over reduced Ag/TiO_2 catalyst in the presence of oxygen and NaOH.

Based on the mechanism proposed in Figure 5, the decrease in FF conversion from 100 to 80%, when atmospheric pressure was used instead of 15 bar air can be explained by the presence of hydrogen on the surface of silver which cannot be removed without oxygen. The catalytic cycle is closed by oxygen, which removes the hydrogen from the surface of Ag through the formation of water and regenerates the Ag catalyst by releasing the active sites to catalyze the further dehydrogenation step. A similar explanation can be concluded when 15 bar of N_2 was used, which explains the lower conversion obtained (17% after 3 h, Figure 4). Without oxygen the surface of silver is covered by adsorbed H-species and the catalytic cycle is broken and further furfural conversion is stopped.

Finally, it is worth noting that for the first-time high yields to furoic acid were obtained at room temperature. Generally, this reaction is carried out on gold nanoparticles at higher temperature [15,17].

2.3. Effect of Base: Nature and Ratio

The effect of OH^- :FF molar ratio (0.25–3) on FF conversion and FA yield (Table 1) was studied at 25 °C under 15 bar of air in the presence of a Ag/TiO_2 catalyst. As expected, no furfural conversion was observed in the absence of a base. However, as the molar ratio OH^- :FF increased from 0.25 up to 1, FF conversion and FA yield increased from 10 to 96%. In the whole OH^- :FF range, the carbon balance was higher than 98 % and the only detected product was FA. By further increasing the amount of base from 1 to 3 equivalents, FF conversion remained constant (~100%) and the FA yield decreased from 96 to 70%. This result is consistent with the observations made during the aqueous phase oxidation of HMF (5-hydroxymethyl furfural) to HMFCFA (5-hydroxymethyl-2-furan-carboxylic acid) over Ag/ZrO_2 catalyst in the presence of NaOH [23]. The authors observed that at 50 °C, as the amount of NaOH increased from 0.5 to 1 equivalent, HMF conversion and HMFCFA yield were also increased. The authors also showed that by increasing the amount of base to two equivalents, the HMF conversion remained constant but the HMFCFA yield decreased.

Table 1. FF conversion, FA yield, and carbon balance in the oxidation of FF over Ag/TiO₂. Reaction conditions: 11.5 mg Ag/TiO₂, n_{FF}/n_{Ag} = 300, C_{0(FF)} = 0.1 mol L⁻¹, 15 bar air, T = 25 °C, 600 rpm, 3 h reaction. NaOH was used as a base.

OH ⁻ :FF Molar Ratio	FF Conversion (%)	FA Yield (%)	Carbon Balance (%)
0.00	0	0	0
0.25	10	10	100
0.50	63	61	98
1.00	96	96	99
3.00	100	70	70

In addition to NaOH, some mild bases were also examined in the selective oxidation of FF (Table 2). Almost no catalytic activity was observed in the presence of NaHCO₃ as in the case without the addition of a base. Na₂CO₃ slightly accelerated the oxidation reaction resulting in 7% conversion of FF after 3 h. This is in agreement with observations made during the liquid phase oxidation of ethylene glycol to glycolic acid over Pt/CeO₂ catalyst in the presence of different bases [24]. It was shown that NaOH was the best base and the others (NaHCO₃ and Na₂CO₃) had a poisoning effect caused by the introduction of HCO₃⁻ and CO₃²⁻ in the reaction medium [24]. In addition, the increase in the base strength represents an increase in the overall concentration of HO⁻ and, consequently, can explain the differences observed in the reaction rate. During the oxidation of aldehydes in basic aqueous solution, the reversible hydration of the aldehyde to geminal diols is a main step. This step is accelerated at a high pH. The geminal diols will adsorb in the metal surface to form an alkoxide that later undergoes a β-elimination to form carboxylic acid. Thus, the combination of high concentration of OH⁻ and/or longer reaction times favours the oxidation of furfural to furoic acid [25].

Table 2. Effect of the nature of the base on FF conversion, FA yield, and carbon balance in the oxidation of FF over Ag/TiO₂. Reaction conditions: C_{0(FF)} = 0.1 mol L⁻¹, n_{FF}/n_{Ag} = 300, n_{base}/n_{FF} = 1, 15 bar of air, T = 25 °C, 600 rpm, 3 h reaction.

Base	FF Conversion (%)	FA Yield (%)	Carbon Balance (%)
No base	0	0	0
NaHCO ₃	1	1	99
Na ₂ CO ₃	7	7	100
NaOH	96	96	99

2.4. Recyclability Tests

The recyclability of the Ag/TiO₂ catalyst was investigated at 25 °C under 15 bar of air using NaOH as a base (Figure 6). In the first run, 83% conversion of FF was achieved with an 82% yield of FA after 2 h of reaction. Before the second and the third runs, the catalyst was recovered by centrifugation and dried overnight at 110 °C without any further activation. A decrease in the catalytic activity was observed and a conversion of 52% was observed during the third run. The carbon balance was always higher than 99% and FA was the only product analyzed by HPLC analysis. No leaching of Ag was detected by ICP analysis of the liquid solution at the end of each run, which does not explain the decrease in the catalytic activity over the Ag/TiO₂ catalyst. The average particle size measured by TEM on Ag/TiO₂ increased from 1.82 nm in the fresh catalyst (Figure 2) to 5.29 nm in the spent catalyst (Figure 7) which could explain the deactivation of the silver catalyst after 3 runs of the reaction.

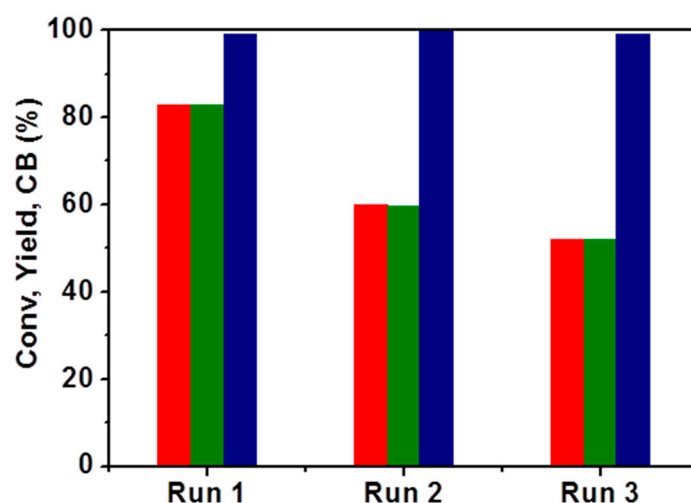


Figure 6. Recyclability study of Ag/TiO₂ catalyst. (■) FF conversion, (■) Yield of FA; (■) Carbon balance: Reaction condition: 11.5 mg Ag/TiO₂, C_{0(FF)} = 0.1 mol L⁻¹, n_{FF}/n_{Ag} = 300, n_{OH⁻}/n_{FF} = 1, 15 bar of air, T = 25 °C, 600 rpm, 2 h reaction; red: FF conversion, green: FA yield, blue: carbon balance.

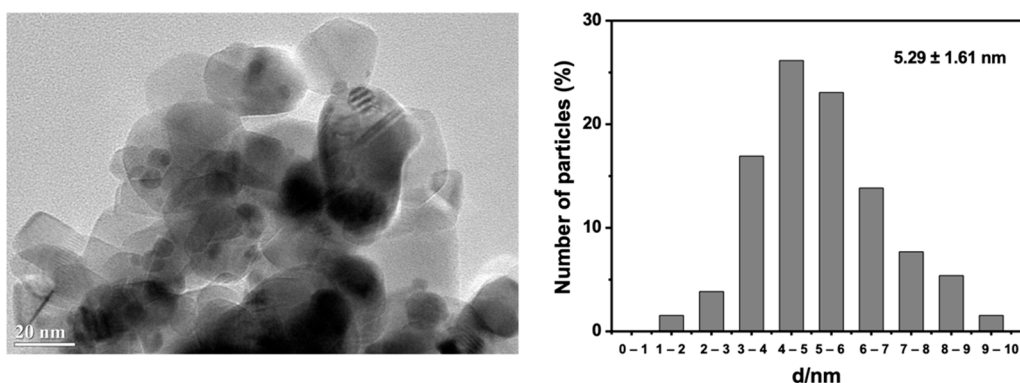


Figure 7. Representative TEM images and size distributions of the spent Ag/TiO₂ catalyst.

Another possibility was the re-oxidation of the catalyst during the drying step. The catalytic test with the calcined (AgO/TiO₂) catalyst was performed and the activity of this catalyst was much lower than that of the reduced one (14% vs. 96% conversion after 3 h). This also demonstrated that the metallic silver was the active phase in this reaction.

3. Materials and Methods

3.1. Catalyst Preparation

Commercial TiO₂-P25, (Sigma Aldrich, Saint Louis, MI, USA), was used as the support. Supported silver catalysts were prepared by a simple impregnation method. It was conducted by introducing the support and a solution of AgNO₃ (50 mM, in water and ethanol at a volume ratio of 1:1) in a flask. The reducing agent sodium borohydride (NaBH₄) was added in excess and the solution was stirred at 30 °C for 4 h. After filtration, the material was washed and dried overnight at 90 °C under static air.

3.2. Characterization of Catalysts

The elemental analysis of Ag and Ti in solutions was performed by ICP-OES (Inductively Coupled Plasma Optical Emission Spectrometry) analysis by using Agilent 720-ES ICP-OES equipment combined with Vulcan 42S automated digestion system (Agilent, Santa Clara, CA, USA). Powder X-ray diffraction patterns (XRD) of the samples were recorded in ambient conditions using a Bruker AXS D8 Advance diffractometer equipped with a nickel filter, a copper tube ($\lambda K\alpha$ (Cu) = 1.54184 Å), and a multi-channel fast detector. Samples

were scanned at $0.014^\circ \text{ s}^{-1}$ over the range $5 \leq 2\theta \leq 80^\circ$ (Bruker, Billerica, MA, USA). The BET specific surface area, pore volume, and pore size distribution were determined from the N_2 adsorption/desorption at -196°C using a TriStar II Plus and 3Flex apparatus Micromeritics (Norcross, GA, USA). Before the measurements, catalysts were degassed at 110°C for 2 h. Transmission electron microscopy (TEM) images were obtained by using a Tecnai G2 20 microscope equipped with a LaB_6 filament and operating at 200 kV (Tecnai, Hillsboro, OR, USA), also equipped with an EDX detector and a GATAN CCD camera (Orius SC1000A, Gatan Inc., Pleasanton, CA, USA). The images were acquired in the parallel beam TEM mode.

3.3. Catalytic Testing

The oxidation of *FF* (Merck, <99%) was carried out in a 30 mL Top Industry autoclave. A total of 20 mL of furfural aqueous solution (concentrations 100 mmol L^{-1}) and 11.5 mg of catalyst were loaded into the reactor. The base (NaOH) was added to the reactor (variable quantity depending on the performed test). In the nature of the base studies the OH to *FF* molar ratio was kept constant (equal to 1). After sealing, the autoclave was purged 3 times with air, pressurized with air to the required pressure ($P_{\text{air}} = 15 \text{ bar}$), and finally heated to the reaction temperature ($T = 25\text{--}110^\circ \text{C}$) under stirring (600 rpm). During the experiment, liquid samples were collected to follow the kinetics of the reaction. At the end of the reaction, air was released, the reactor was cooled, and the catalyst was collected by centrifugation. At the end of each reaction, the aqueous solution was analyzed by ICP to detect the leaching of metals expressed in ppm. A blank test was performed without a catalyst and no conversion of *FF* was observed.

The reaction products were analyzed by High Performance Liquid Chromatography (HPLC, Waters 2410 RJ, Waters, Milford, MA, USA) equipped with RI and UV ($\lambda = 253 \text{ nm}$) detectors and a Rezex ROA–organic Acid H^+ column ($\text{Ø } 7.8 \text{ mm} \times 300 \text{ mm}$) at 25°C . Diluted H_2SO_4 (5 mmol L^{-1} , 0.5 mL min^{-1}) was used as the mobile phase. The products were identified by their retention times compared to available standards that were also used to determine the response factors.

The conversion of *FF* at time t was calculated from Equation (1):

$$\text{Conversion}_t(\%) = \frac{C_0^{FF} - C_t^{FF}}{C_0^{FF}} \times 100 \quad (1)$$

where C_0^{FF} is the initial concentration of *FF* and C_t^{FF} is the concentration of *FF* at time t . The yield and selectivity to *FA* were calculated using Equations (2) and (3), respectively.

$$\text{Yield}_t^{FA}(\%) = \frac{C_t^{FA}}{C_0^{FF}} \times 100 \quad (2)$$

$$\text{Selectivity}_t^{FA}(\%) = \frac{C_t^{FA}}{(C_0^{FF} - C_t^{FF})} \times 100 \quad (3)$$

in which C_t^{FA} is the concentration of *FA* at time t .

The carbon balance (CB) at time t was calculated according to Equation (4).

$$\text{Carbon balance (CB)} = \frac{C_t^{FF} + C_t^{FA}}{C_0^{FF}} \times 100 \quad (4)$$

where C_0^{FF} is the initial concentration of *FF* (in mol L^{-1}) and C_t^{FA} is the concentration of *FA* at time t (in mol L^{-1}).

At the end of each reaction, in order to detect the leaching of silver (in ppm), ICP analyses of the aqueous solution were performed.

4. Conclusions

The TiO₂-supported Ag catalyst prepared by the simple impregnation method was proven to have an excellent activity in the oxidation of furfural. A high yield of furoic acid was obtained in an alkaline aqueous solution, under 15 bar of air and room temperature. The effect of different reaction parameters including temperature (25–110 °C), effect of atmosphere, base equivalent ($n_{\text{OH}^-} / n_{\text{FF}} = 0.25\text{--}3$), and nature of the inorganic base used (NaOH, NaHCO₃, and Na₂CO₃) on catalytic activity and yield were studied. Whatever the reaction conditions, furoic acid was the only product detected. The catalytic activity of Ag/TiO₂ catalyst however declined after three runs of the reaction which is associated with both an increase in the size and the re-oxidation of the silver particles.

Author Contributions: A.S.: conceptualization, data curation, formal analysis, writing—original draft, R.W.: conceptualization, project administration, supervision, writing—original draft, writing—review and editing, S.P.: reviewing. All authors have read and agreed to the published version of the manuscript.

Funding: This research received no external funding.

Data Availability Statement: The data presented in this study are available on request from the corresponding author.

Acknowledgments: Chevreul Institute (FR 2638), Centrale Lille Institute, Ministère de l'Enseignement Supérieur, de la Recherche et de l'Innovation, Hauts-de-France Région and European Regional Development Fund (ERDF) are acknowledged for their financial support to this work.

Conflicts of Interest: The authors declare no conflict of interest.

References

1. Alonso, D.M.; Bond, J.Q.; Dumesic, J.A. Catalytic Conversion of Biomass to Biofuels. *Green Chem.* **2010**, *12*, 1493–1513. [[CrossRef](#)]
2. Besson, M.; Gallezot, P.; Pinel, C. Conversion of Biomass into Chemicals over Metal Catalysts. *Chem. Rev.* **2014**, *114*, 1827–1870. [[CrossRef](#)] [[PubMed](#)]
3. Ruppert, A.M.; Weinberg, K.; Palkovits, R. Hydrogenolysis Goes Bio: From Carbohydrates and Sugar Alcohols to Platform Chemicals. *Angew. Chem. Int. Ed.* **2012**, *51*, 2564–2601. [[CrossRef](#)]
4. Pothu, R.; Gundebayina, R.; Boddula, R.; Perugopu, V.; Ma, J. Recent advances in biomass-derived platform chemicals to valeric acid synthesis. *New J. Chem.* **2022**, *13*, 5907–5921. [[CrossRef](#)]
5. Bozell, J.J.; Petersen, G.R. Technology Development for the Production of Biobased Products from Biorefinery Carbohydrates—the US Department of Energy's "Top 10" Revisited. *Green Chem.* **2010**, *12*, 539–554. [[CrossRef](#)]
6. Murzin, D.Y.; Bertrand, E.; Tolvanen, P.; Devyatkov, S.; Rahkila, J.; Eränen, K.; Wärnå, J.; Salmi, T. Heterogeneous Catalytic Oxidation of Furfural with Hydrogen Peroxide over Sulfated Zirconia. *Ind. Eng. Chem. Res.* **2020**, *59*, 13516–13527. [[CrossRef](#)]
7. Lange, J.-P.; van der Heide, E.; van Buijtenen, J.; Price, R. Furfural—A Promising Platform for Lignocellulosic Biofuels. *ChemSusChem* **2012**, *5*, 150–166. [[CrossRef](#)]
8. Delbecq, F.; Wang, Y.; Muralidhara, A.; El Ouardi, K.; Marlair, G.; Len, C. Hydrolysis of Hemicellulose and Derivatives—A Review of Recent Advances in the Production of Furfural. *Front. Chem.* **2018**, *6*, 146. [[CrossRef](#)]
9. Drault, F.; Snoussi, Y.; Thuriot-Roukos, J.; Itabaiana, I.; Paul, S.; Wojcieszak, R. Study of the Direct CO₂ Carboxylation Reaction on Supported Metal Nanoparticles. *Catalysts* **2021**, *11*, 326. [[CrossRef](#)]
10. Drault, F.; Snoussi, Y.; Paul, S.; Itabaiana, I.; Wojcieszak, R. Recent Advances in Carboxylation of Furoic Acid into 2,5-Furandicarboxylic Acid: Pathways towards Bio-Based Polymers. *ChemSusChem* **2020**, *13*, 5164–5172. [[CrossRef](#)]
11. Eseyin, A.E.; Steele, P.H. An Overview of the Applications of Furfural and Its Derivatives. *Int. J. Architect. Comput.* **2015**, *3*, 42. [[CrossRef](#)]
12. Arias, P.L.; Cecilia, J.A.; Gandarias, I.; Iglesias, J.; López Granados, M.; Mariscal, R.; Morales, G.; Moreno-Tost, R.; Maireles-Torres, P. Oxidation of Lignocellulosic Platform Molecules to Value-Added Chemicals Using Heterogeneous Catalytic Technologies. *Catal. Sci. Technol.* **2020**, *10*, 2721–2757. [[CrossRef](#)]
13. Zeitsch, K.J. The Chemistry and Technology of Furfural and Its Many By-Products. *Elsevier B* **2000**, *13*, 159–163.
14. Xu, C.; Paone, E.; Rodríguez-Padrón, D.; Luque, R.; Mauriello, F. Recent Catalytic Routes for the Preparation and the Upgrading of Biomass Derived Furfural and 5-Hydroxymethylfurfural. *Chem. Soc. Rev.* **2020**, *49*, 4273–4306. [[CrossRef](#)] [[PubMed](#)]
15. Ferraz, C.P.; Costa, N.J.S.; Teixeira-Neto, E.; Teixeira-Neto, Â.A.; Liria, C.W.; Thuriot-Roukos, J.; Machini, M.T.; Froidevaux, R.; Dumeignil, F.; Rossi, L.M.; et al. 5-Hydroxymethylfurfural and Furfural Base-Free Oxidation over AuPd Embedded Bimetallic Nanoparticles. *Catalysts* **2020**, *10*, 75. [[CrossRef](#)]
16. Taarning, E.; Nielsen, I.S.; Egeblad, K.; Madsen, R.; Christensen, C.H. Chemicals from Renewables: Aerobic Oxidation of Furfural and Hydroxymethylfurfural over Gold Catalysts. *ChemSusChem* **2008**, *1*, 75–78. [[CrossRef](#)]

17. Roselli, A.; Carvalho, Y.; Dumeignil, F.; Cavani, F.; Paul, S.; Wojcieszak, R. Liquid Phase Furfural Oxidation under Uncontrolled PH in Batch and Flow Conditions: The Role of In Situ Formed Base. *Catalysts* **2020**, *10*, 73. [[CrossRef](#)]
18. Menegazzo, F.; Manzoli, M.; di Michele, A.; Ghedini, E.; Signoretto, M. Supported Gold Nanoparticles for Furfural Valorization in the Future Bio-Based Industry. *Top. Catal.* **2018**, *61*, 1877–1887. [[CrossRef](#)]
19. Tian, Q.; Shi, D.; Sha, Y. CuO and Ag₂O/CuO Catalyzed Oxidation of Aldehydes to the Corresponding Carboxylic Acids by Molecular Oxygen. *Molecules* **2008**, *13*, 948–957. [[CrossRef](#)]
20. Schade, O.R.; Gaur, A.; Zimina, A.; Saraçi, E.; Grunwaldt, J.-D. Mechanistic Insights into the Selective Oxidation of 5-(Hydroxymethyl)Furfural over Silver-Based Catalysts. *Catal. Sci. Technol.* **2020**, *10*, 5036–5047. [[CrossRef](#)]
21. Farfan-Arribas, E.; Madix, R.J. Characterization of the Acid–Base Properties of the TiO₂ (110) Surface by Adsorption of Amines. *J. Phys. Chem. B* **2003**, *107*, 3225–3233. [[CrossRef](#)]
22. Davis, S.E.; Zope, B.N.; Davis, R.J. On the Mechanism of Selective Oxidation of 5-Hydroxymethylfurfural to 2,5-Furandicarboxylic Acid over Supported Pt and Au Catalysts. *Green Chem.* **2012**, *14*, 143–147. [[CrossRef](#)]
23. Schade, O.R.; Kalz, K.F.; Neukum, D.; Kleist, W.; Grunwaldt, J.-D. Supported Gold- and Silver-Based Catalysts for the Selective Aerobic Oxidation of 5-(Hydroxymethyl)Furfural to 2,5-Furandicarboxylic Acid and 5-Hydroxymethyl-2-Furancarboxylic Acid. *Green Chem.* **2018**, *20*, 3530–3541. [[CrossRef](#)]
24. Shi, H.; Yin, X.; Subramaniam, B.; Raghunath, V.C. Liquid-Phase Oxidation of Ethylene Glycol on Pt and Pt–Fe Catalysts for the Production of Glycolic Acid: Remarkable Bimetallic Effect and Reaction Mechanism. *J. Catal.* **2019**, *58*, 18561–18568. [[CrossRef](#)]
25. Ferraz, C.; Garcia, M.; Teixeira-Neto, E.; Rossi, L. Oxidation of benzyl alcohol catalyzed by gold nanoparticles under alkaline conditions: Weak vs. strong bases. *RSC Adv.* **2016**, *6*, 25279–25285. [[CrossRef](#)]